Lightning Impulse Current Tests on Conductive Fabrics

Jorge Alejandro Cristancho, Carlos A. Rivera G., Jorge E. Rodriguez M., John J. Pantoja A., Liz K. Herrera Q., Francisco Roman

Lightning Impulse Current Tests on Conductive Fabrics

Jorge A. Cristancho C.[*,1], Carlos A. Rivera G. [1], Jorge E. Rodriguez M. [1], John J. Pantoja A. [1], Liz K. Herrera Q. [2], Francisco J. Román C.[+,1]

[1]Electromagnetic Compatibility Research Group EMC-UN
[2]Grupo de análisis de falla, integridad y superficie AFIS
Universidad Nacional de Colombia
Bogotá D.C., Colombia

* jacristanchoc@unal.edu.co, + fjromanc@unal.edu.co

Abstract

The large amount of electric current associated to lightning discharges is hazardous for living beings, equipment, structures and buildings. To protect those targets against lightning are used Lightning Protection Systems (LPS). However, there are some temporary outdoor activities and backcountry places where an adequate LPS cannot be set up mainly due to the large dimensions of its components and its heavy weight. On the search of light weight lightning protection materials that can be used as part of special LPS, we research some types of electroconductive fabrics by applying high lightning impulse currents in laboratory. The fabric samples checked were pieces of 10 cm x 10 cm: two rip-stop type, a plain-weave, a non-woven and a carbon-impregnated polymeric, all of them obtained commercially. Under laboratory conditions, these samples were subject to subsequent lightning impulse currents registering the voltage and current signals. Optical and scanning electron microscope inspections were performed after tests. Despite some changes visualized as marks left on the fabric surface, the results show that investigated conductive textiles can endure ground currents produced by atmospheric lightning since they withstand the several applied laboratory lightning impulse currents. The outcomes suggest that the weave pattern of the conductive fabric influences the lightning current tolerance, enabling some conductive fabrics to be used in heavy-current applications and as part of personal LPS for outdoor, backcountry and mobile shelters, particularly when lightweight and portability are mandatory.

Keywords

Lightning protection, conductive fabrics, high-current tests, tents, shelters

Introduction

Due to the uneven distribution of lightning activity on the planet, global lightning maps show that some places in the world have high levels of lightning activity. In these places, the population is more prone to suffer injuries caused by lightning. The top 100 places of the world with the highest lightning activity have a lightning density in a range between 83,45 and 232,52 flashes/km^2 [1]. Colombia, placed in northwestern South America, has 7 of the top 10 lightning hotspots of South America [1], with an accordingly elevated rate of lightning related accidents on living beings. 757 lightning-caused human fatalities in the period of 2000 to 2009 were reported in Colombia, which is an alarming figure mainly considering that statistics in this country are underestimated [2]. Several accidents reported by both, the media and the technical literature, show some particular groups of people that are more vulnerable to the risk of lightning, particularly those involved in outdoor activities or placed in open fields [2]–[5]. The Colombian Army has reported 72 dead and 210 injured soldiers by lightning accidents in the time period from 2003 to 2012 [6].

In order to reduce the risk of damage caused by lightning strikes on living beings, structures, buildings, installations and their contents [7], there are several techniques intended to intercept direct lightning flashes and to conduct and disperse their currents safely into the earth [8]. Therefore, to prevent injury of living beings and damage to buildings, equipment and systems, a lightning protection system (LPS) should be able to capture and divert safely the hazardous impulsive lightning currents into the ground. For fixed external building protection, the IEC62305 and NFPA 780 [7], [9] recommend the use of some materials and components that are heavy and bulky in most of the cases. Nevertheless, in some outdoor, faraway, backcountry or not easily accessible locations, the use of weighty materials and equipment is almost impossible, constraining the possibility to have acceptable LPSs. This condition makes some human activities permanently exposed to the catastrophic risk of lightning.

Mobile shelters, temporal campsites and other open field sites require protection systems against lightning, but the outdoor conditions demand easy-to-use and lightweight equipment. Some reports with nonfatal victims suggest that certain light metallic elements could have helped to save the life of lightning struck people [3], [10]. Nevertheless, it is necessary to analyze the existing information and carry out laboratory tests to establish what light materials could safely divert the high currents produced by electrical atmospheric discharges.

Through lightning impulse current tests, to simulate lightning strokes, and microscopy observations, we assess certain types of electrically conductive textiles, intended for shielding of electromagnetic fields, as possible light weight LPS to be applied on tents, mobile shelters and other power applications. In this paper, we show the main outcomes of these tests and observations.

Overview of electroconductive fabrics

Technical textiles are used in many applications and classified according to their end use. For the Techtextil Exhibition Trade Fair, the Messe Frankfurt Group divided the show into 12 application areas [11], which are the current accepted classification for technical textiles. The “Protech” category includes the developments in personal and property protective textiles such as fabrics that can conduct electric currents, primarily intended for their use in antistatic, medical and EMI shielding protective military and civil applications.

Conductive fabrics

There are a wide range of electrically conductive fiber-based textile products with different specific electrical conductivities [12]. Electroconductive fabrics are made with fibers, yarns or threads made from conductive, low conductive, or non-conductive substrates coated or embedded with electrically conductive elements such as nickel, copper or silver. Depending on the application, other metallic materials or alloys are used (such as gold, steel or titanium), as well as non-metallic ones (e.g. conductive polymers, carbonaceus or graphenes) [13], [14]. Fig. 1 shows a typical structure of an electroconductive monofilament yarn and a micrograph of a woven conductive fabric made of multifilament yarns. Each single yarn has a fiber core of a non-conductive material coated with an outer conductive layer (in this case, inner polyester with two outer metal layers). The last polymer coating is for coloring and anticorrosion purposes. Fabrics made with inner polymer yarns with metallic coatings constitute one of the most popular products in the 2015 conductive fabrics market since these yarns can be fabricated by a simple metal-deposition treatment [15].

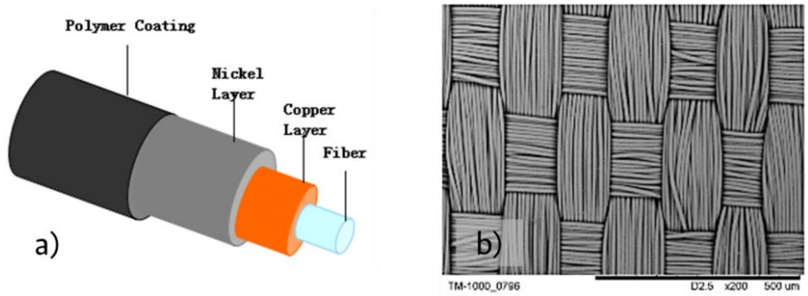

Figure 1. Structure of a electroconductive yarn (a) and a micrograph of a conductive fabric (b) [16].

An electrically conductive, electroconductive or just conductive fabric, can be defined as a network of conducting interlaced yarns arranged according to a given pattern. Each conductive yarn drives electrical signals in the network, transmitting them from one point to another, and can be designed to follow a given electrical circuit [17]. Normally these electrical signals are of low power. However, it will be shown that some of them were subjected to high current impulses, such as laboratory lightning impulse currents, and could withstand natural atmospheric lightning currents.

There are several types of conductive fabrics depending on its weave pattern (woven, non-woven or knitting, the latter is not treated in this work), base material, conductive and coating materials and layers, number of plies, number of conductive yarns, thickness, weight etc. Fig. 2 shows micrographs of three common conductive fabrics revealing the weave pattern: (a) is a woven rip-stop, (b) is a plain-weave and (c) is a non-woven fabric. These textiles are made with fibers formed by electrically insulating core of polyester, metalized with an outer nickel-cooper layer. The structure of both woven (a and b) and non-woven (c) fabrics shows a clear difference, with a defined pattern for the woven type in contrast to the random layout of the nonwoven one.

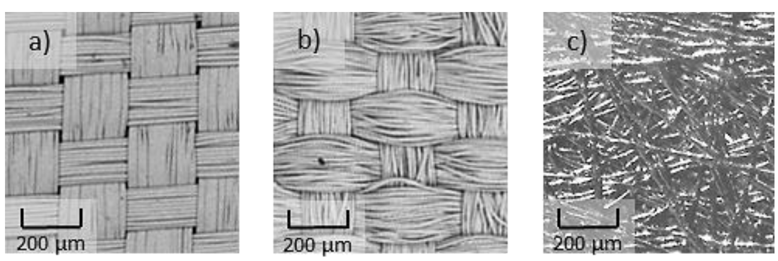

Figure 2. Micrographs of three conductive fabrics: ripstop (a), plain weave (b) and nonwoven (c).

On the one hand, woven fabrics consist of interlacements of yarns in mutually perpendicular directions, as showed in Fig. 2 a) and b), interlacing or interweaving warp-and-weft yarns. On the other hand, non-woven fabrics are textiles whose structure is produced by the bonding or interlocking of fibers with mechanical, chemical, thermal or solvent methods, or combinations thereof [14]. Micrographs of Fig. 2 correspond to electroconductive fabric samples. The weave structure, pattern and the number of yarns depends on the fabric type. Fig. 3 shows an optical micrograph of the warp cross section of a rip-stop electroconductive fabric showing the 48 weft yarns of the textile. Each yarn has an average 15 μm diameter with an outer conductive layer of about 1 μm thickness.

Commonly, the warp yarns are more stressed than the weft, since the former are stretched to receive the interlaced ones of the latter.

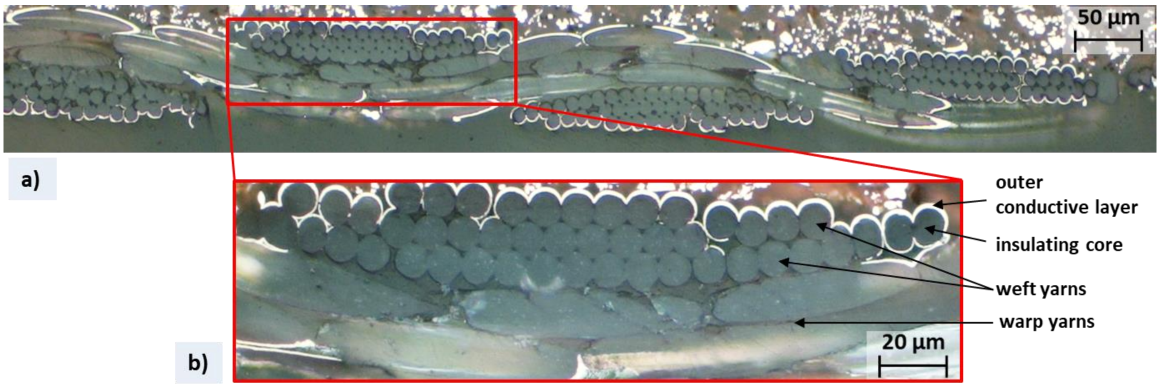

Figure 3. Optical microscopy observations of a warp cross-section of an electroconductive rip-stop fabric showing 48 weft yarns cramped along warp fibers (a). In the zoom image (b) in the external layer is possible to identify the inner insulating fibers with the outer conductive layer.

Sheet resistance

Conductive fabrics cannot be considered as homogeneous structures with isotropic electrical current distribution. Electrical modeling of conductive textiles is difficult, since the material must be treated as a combination of resistors in series and parallel connections considering the interlacing fibers [18]. Fig. 4 a) shows a representation of a simple plain-weave section model of two warp and two weft interlaced yarns (on blurry image) with the electrical equivalent model superimposed. An electrical model of the whole conductive fabric could be treated as a very large-scale symmetric network of basic yarn interconnected sections as previously shown. The entire model can be reduced to multiple single yarns connected in parallel [19] which in the end can be taken as a uniform conductive sheet (Fig. 4 b). The resistance of a full symmetric grid (a square of fabric, independent of the side length) corresponds to that of the basic electric model.

The resistivity of the conductive coating materials determines the electrical resistance of the yarns (R) and the contact-resistance (Rc) between the interlaced fibers, therefore, of the entire fabric. The electrical resistance value will also depends on several external factors, such as temperature, humidity, pressure or extension [18], [20]. Then, considering the conductive textile surface as a thin film conductor, the sheet resistance – sometimes called surface resistivity – is frequently used to refer to their electrical resistance, different from the bulk resistance used for wires conductor specification. Considering Fig. 4 b), the regular three-dimensional resistance of a conductor can be written as in Eq. (1) which becomes Eq. (2) for a square of sides *w* and thickness *t*, in the current direction *I*, going through the cross-sectional area *A*.

$$R = \rho \frac{Lenght}{Area} \qquad (1)$$

$$R = \rho \frac{W}{t.W} = \frac{\rho}{t}\frac{W}{W} = \frac{\rho}{t} \;\; [\Omega] \qquad (2)$$

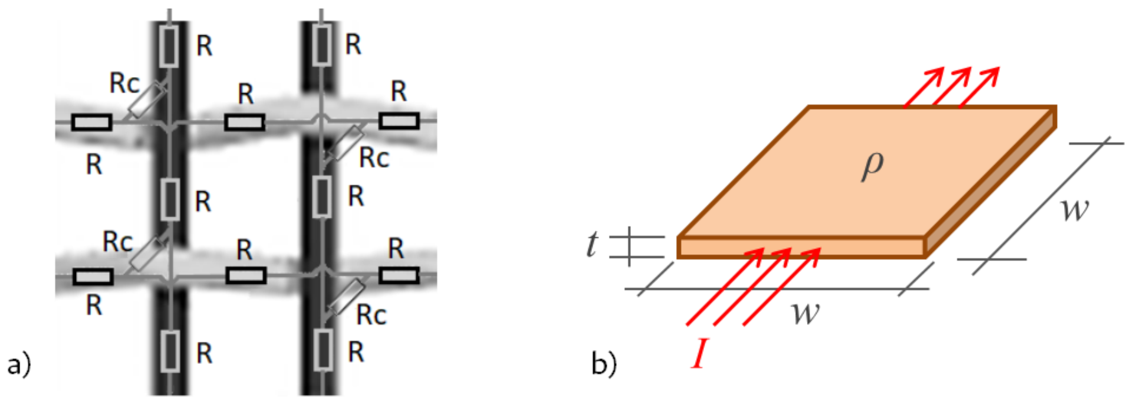

Figure 4. An equivalent basic electric model for a fabric section with R as the yarn resistance and Rc as the contact resistance between warp and weft yarns (a), and a simplified surface geometry considered for the sheet resistance estimation of a square of film conductor (b).

Equation (2) is valid for a square of film conductor, where $\frac{\rho}{t}$ is the so-called sheet resistance *Rsh*, commonly expressed in units of ohms per square (Ω/□), which emphasizes the fact that the resistance measured is over a square of material and it is independent of the side length [13], [21], [22].

Overview of lightning impulse tests

A lightning flash to earth is an electrical discharge of atmospheric origin between cloud and earth consisting of one or more strokes [7]. Cloud-to-ground lightning effects depends mainly on the high current amplitudes developed when the unbalanced opposite charges between clouds and ground are neutralized. When a lightning strikes the ground directly or through a tall object, the currents are distributed on the earth from the striking point to outside. Despite of lightning currents could reach more than 200 kA, for negative first strokes the global lightning median return-stroke peak current is about 30 kA and typically 12 kA for subsequent strokes [23]. However, for some countries such as Brazil, Colombia and Rhodesia the average lightning peak value is about 42 kA [23], [24]. The lightning current diverted into the ground gives lower values as the current density decreases, although it is still hazardous to life and health. Laboratory lightning impulse current tests are used to simulate natural lightning currents to assess the effects of impulsive currents over equipment and materials.

Parameters of lightning impulses

The peak value I, the front time T_1 and the time to half value T_2 are basic parameters of the standardized wave shape typically used in laboratories to simulate the effects of lightning currents on LPS components [7] as shown in Fig. 5. Commonly, in a lightning impulse the time T_2 is less than 2 ms. When it is talked about a 20 kA 4/10 µs current wave-shape, it refers to a current signal of 20 kA peak, 4 µs of front time and 10 µs of tail time to their half value of 10 kA. In the same way, an impulse current of 10 kA 8/20 µs indicates a signal with 10 kA of peak, 8 µs of front time and 20 µs to 50% peak value at the tail, i.e. 5 kA.

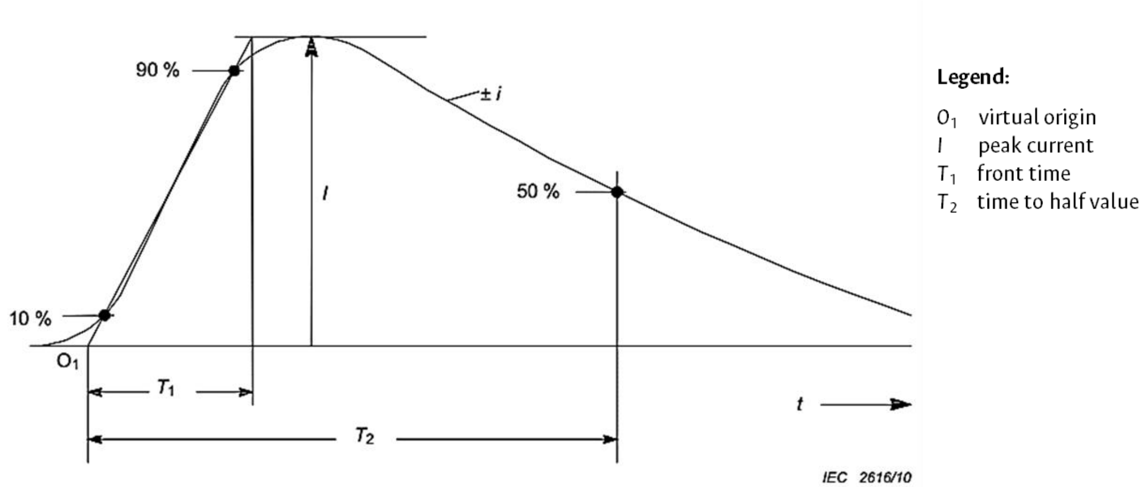

Figure 5. A standard lightning impulsive current with its parameters according to IEC 62305 series [7].

Energy dissipated as Joule heating

When an electrical current flow through a resistive material it is produced heating due to the Joule effect. For the estimation of the energy dissipated by the conductive fabric as joule heating due to each applied current pulse, the instantaneous power applied over the electroconductive fabric should be considered. The following expressions (2) and (3) are used to evaluate the energy after each current impulse:

$$P(t) = V_e(t) \cdot I(t) = (I(t) \cdot R) \cdot I(t) = I^2(t) \cdot R \quad (2)$$

$$E = \int_{t=0}^{T} P(t)dt = R \cdot \int_{t=0}^{T} I^2(t)dt \quad (3)$$

where *P* is the power, *Ve* is the measured voltage between electrodes, *I* the current applied, *R* the resistance of the conductive fabric, *E* the energy, and *t* is the time.

Setup and methodology

Following the methodology reported in Cristancho *et al.*, 2018 [25], sample conductive fabric tests were conducted over three samples of four different textile types and one carbon-impregnated polymeric commercial film. The samples of 10 cm by 10 cm of the four weave types, named as F1 to F4, were individually subjected to a set of at least four subsequent lightning impulse currents. Each set of impulses starts from 5 kA, increasing in leaps of about 4 kA with time intervals of 5 minutes between each test. Beside these textile tests, a polymeric film (F5) was also tested in a similar way but only with a lightning impulsive current of 5 kA. In all these tests, the current was applied through copper clamp electrodes, lengthwise to the surface of the fabric, in the warp direction.

Additionally, an A-frame type scale shelter model with a ratio of 1:10 made with the F1 conductive fabric was used to perform two lightning impulse tests. The entire base of the scale model was placed over a conductive sheet connected to electrical ground, simulating the soil. Two consecutive 14 kA impulses were applied on the ridge of the modeled shelter, the second one after 5 minutes of the first one. Then, the current flow in this case is different than for the previous squared samples, where the current flow goes from one edge to the other. Here, in the A-frame model, the current goes from the attachment point on the ridge to the grounded base.

Fabrics used as samples under test

Conductive fabrics, come from the same manufacturer, were used as Objects Under Test (OUT). The OUT samples were squared pieces of conductive fabrics of 10 cm x 10 cm of the following weave types: rip-stop (F1), rip-stop with a side layer coated with a flame-retardant composite UL94V-0 (F2), plain-weave (F3) and a non-woven textile (F4). The structure of each yarn of the conductive fabrics follows the description given in Fig. 1, but without the external polymer coating. The inner fiber is a monofilament made of polyester, constituting 65% of the entire yarn. The manufacturer data sheet gives the composition of the remaining 35% outer conductive layer as 57% Cu-43% Ni. The UL94V-0 level flame-retardant coating composite of the F2, covers one side of a conductive rip-stop fabric of the F1 type. The main characteristics of the conductive fabric samples are summarized in Table I. Although the unit of electrical resistance is the ohm (Ω), for thin-film conductors it is common practice to refer to the unit of sheet resistance as ohms per square (Ω/□) [13], [21], [22].

TABLE I. PARAMETERS OF THE TESTED CONDUCTIVE FABRICS AND FILM

Item	Unit	F1	F2	F3	F4	F5
Weave pattern	type	Rip-stop	Rip-stop with FR(a)	Plain	Non-woven	polymeric film
Weight	g/m^2	90±10	245±10	130±10	90±10	238±10
Thickness	mm	0,10±0,01	0,16±0,02	0,15±0,02	0,08±0,01	0,10±0,01
Sheet resistance	Ω/□(b)	≤ 0,05	≤ 0,07	≤ 0,07	≤ 0,05	< 31000
Resistivity	μΩ·m	≤ 5,0±0,5	≤ 11,2±1,4	≤ 10,5±1,4	≤ 4,0±0,5	< 3,1E6±0,1E6
Conductive material	type	Ni-Cu	Ni-Cu(a)	Ni-Cu	Ni-Cu	impregnated with carbon black
Core material	type	polyester	polyester	polyester	polyester	polymeric-film

(a) Uses a side with a coating layer of Flame Retardant level UL94V-0 composite.

(b) Mathematical unit is the ohm, but the common unit used for the sheet resistance is the ohm per square.

Before all the tests, the fabric samples were observed through an optical microscope (Olympus BX-41 with U-CMAD3) and weighted in an analytical balance (Sartorius Entris 224I 1S). After the current test, the samples were observed in the microscope and weighted again to compare the fabrics before and after the tests and to analyze how the fabrics were changed by the high current flow. Additionally, some small sections trimmed out from the samples were examined through a scanning electronic microscope – SEM (Tescan Vega 3 SB with secondary electrons – SE detector and backscattering electrons BSE detector) to increase the observation capacity to identify the structure and type of involved materials, and to get more details of the changes over the fabric surface. All the samples observed in the SEM used an acceleration voltage of 20,0 kV. Moreover, to estimate the elemental composition of the conductive surface layer, SEM with Energy Dispersive Spectrometry

(EDS) analyses were performed over a sample of rip-stop conductive fabric (F1), before and after lightning tests.

The polymeric film F5, with sheet resistance of 31 kΩ/□ and 0,1 mm thickness, was included in Table I but was only tested with a single current impulse, because it ignited and melted along the test electrodes contacts, before allowing other trials. For this reason, F5 was not studied such as the textile samples and it does not appear in most of this paper.

Lightning impulse current generator setup

The OUT samples were tested with four consecutive 8/20 μs impulse currents, starting from 5 kA in increasing leaps greater than 2 kA (up to slightly above the maximum current conduction capacity of the fabric). The lightning impulsive currents were generated by Lightning Impulse Current Generators (LICG) of the Universidad Nacional de Colombia – Campus Bogotá. The tests were performed in the Electrical Tests Lab – LABE and the High Voltage Teaching Lab. Since impulse voltages with front durations varying from less than one up to a few tens of microseconds are considered as lightning impulses [26], the 8/20 μs current waveshapes of the LICG, with 8 μs of front time, can be called as lightning impulse currents.

The schematic setup of the LICG is represented in Fig. 5. By changing the distance between spheres of the spark-gap, it is possible to control the LICG charging voltage, hence the peak amplitude of the applied current pulses. Then, for each of the four consecutive tests, the impulse generator of the LICG was set at a charge voltage to obtain the peak current desired for each discharge. For example, for the fabric F1 were used 2,1; 3,5; 5,0 and 5,7 kV of charge voltage to obtain 5,4; 8,9; 13,0 and 14,9 kA in average. To observe and compare the impedance behavior of each sample, it is necessary to measure and record the voltage and current signals. Through a Rogowski coil with integrator and a High voltage Probe with 1000:1 relation, both current and voltage were measured. To record these signals, they were led to two channels of an Agilent DSO6104A oscilloscope with ground isolation. The conductive fabric as OUT were supported by two copper clamp electrodes to provide physical support and electrical contacts between the current generator and the fabric sample. In this setup, the OUT must have enough low impedance to allow the conduction of the current impulse. If the impedance of the OUT increases, e.g. due to loss of conductive material, up to a high impedance, it can act as an open circuit blocking the impulse current flow. Then, the OUT impedance state determines the effective current applied and the voltage measured.

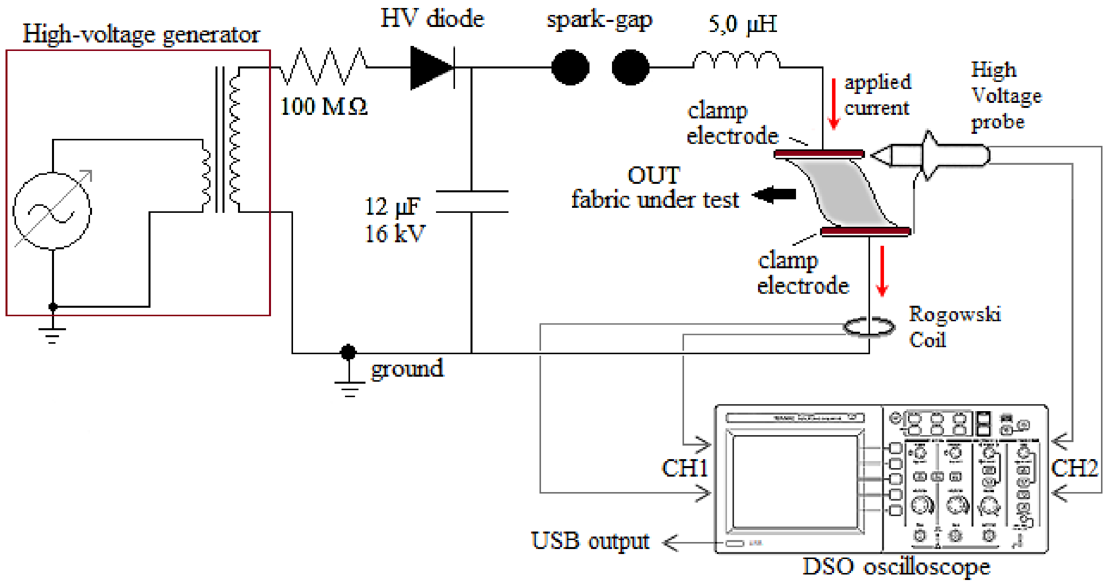

Figure 5. Schematic of the Lightning Impulse Current Generator (LICG) setup used to test the electroconductive fabric samples.

Results

Optical microscopy

Figure 6 shows some micrographs of the untested samples, which illustrate the differences of the weave-type. F1 and F2 correspond to rip-stop type, F3 to plain-weave type and F4 to nonwoven conductive fabrics type. F2 includes a side coated, let us say the back, with a flame-retardant composite that increases the temperature strength, as well as the fabric thickness, stiffness and weight.

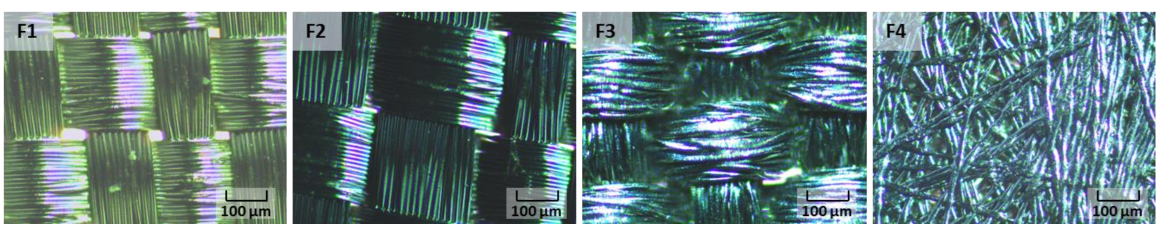

Figure 6. Optical micrographs of the tested conductive fabrics (adapted from [25]).

Lightning current pulse tests

After applying the current pulses over each sample, some patterns appeared on the fabric surface, particularly close to the electrodes. The current and voltage signatures of the fourth lightning impulse current applied to the F4-3 fabric are shown in the upper part of Fig. 7. The lower part of Fig. 7 shows pictures of the OUT surface after the test. In these last two photographs, a horizontal mark perpendicular to the current flow it is clearly observed besides the marks close to the electrodes.

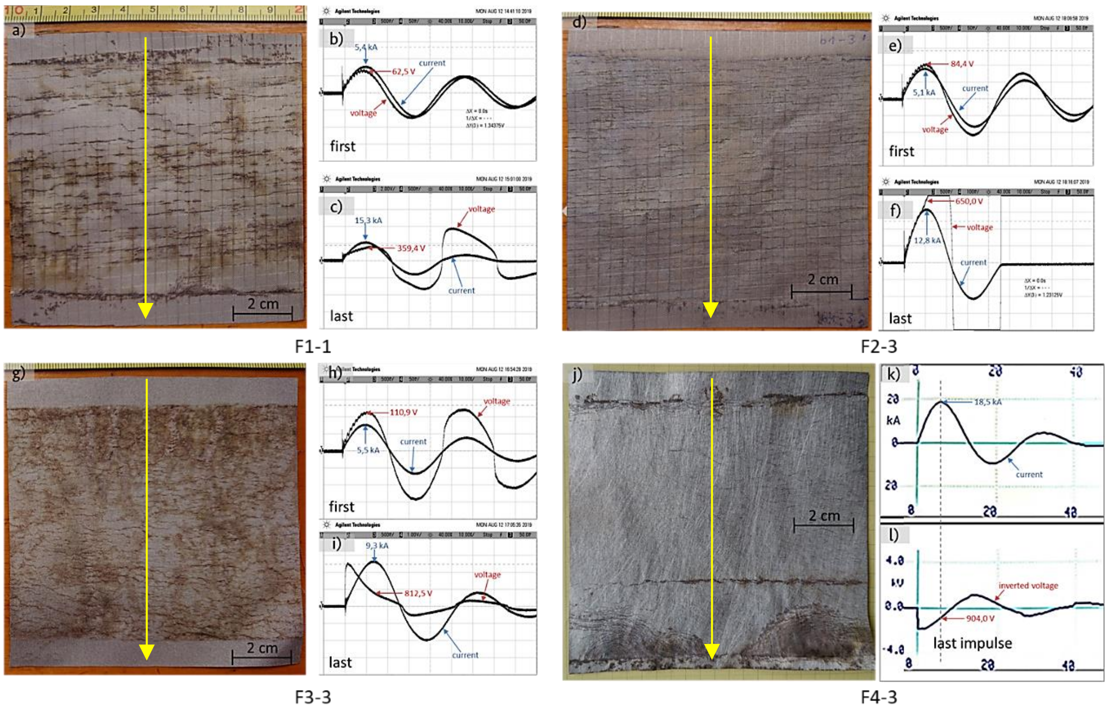

Figure 7. Fabrics after lightning impulse current tests with current and voltage signatures, showing the first and last applied impulses. The voltage signal in F4-3 (l) has negative polarity by the acquisition system conection. It can be noticed dark marks perpendicular to the current flow (yellow arrows) and horizontal scratches on the fabric surfaces.

Fig. 8 shows the voltage-current plots measured on the three fabric samples of each weave pattern. Impulse currents starting form 5 kA, increasing in steps of about 4 kA, were applied for each sample and recorded the voltage between the opposite ends of the fabric sample, i.e. between the electrodes. From the voltage-current plotted tests, it was observed for the first three impulses in all the tests that the voltage-current characteristic is almost constant indicating a linear resistance. This behavior is observed in each of the three samples of each fabric type. The data of the first three current impulses was used to calculate the electrical resistance of the fabric at each current level trial. It was taken the first peak current value and the corresponding voltage to that peak. Using the Ohm's law, the "electrical resistance test" was calculated for each fabric sample and averaged for the weave pattern type as presented in Table II. For example, the non-woven fabric F4 shows a resistance average value of 0,03 Ω, which is consistent with the sheet resistance value given in Table I.

However, the fourth lightning current impulse produced a considerable variation in the electrical behavior of the conductive fabrics. This is most evident for the F3 plain-weave fabric, which had an unexpected change after that, different in the three samples. On the other hand, for the F4 fabric, the last current of 19 kA, produced changes of about 33% and up to 96%. This large variation was not expected from the projections of the previously measured values of the textile resistance.

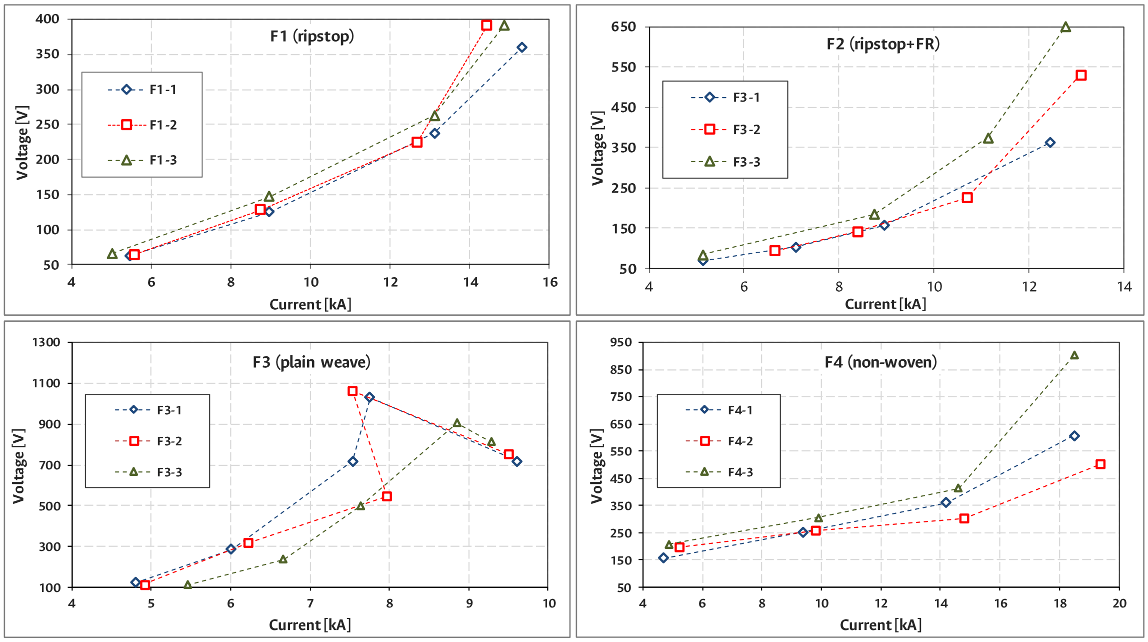

Figure 8. Voltage-Current graphs of the lightning-type current tests with the LICG over the electroconductive fabrics. Each colored line (blue ◊, red □, green Δ) corresponds to the sample tested at the several peak current values for each weave type. Note that horizontal and vertical scales are different in all the graphs.

TABLE II. AVERAGE RESISTANCE FOR THE FIRST THREE IMPULSES OF EACH FABRIC SAMPLE AND AVERAGE FOR EACH WEAVE PATTERN TYPE

Sample	**F1-1**	**F1-2**	**F1-3**	**F2-1**	**F2-2**	**F2-3**	**F3-1**	**F3-2**	**F3-3**	**F4-1**	**F4-2**	**F4-3**
Resistance [Ω]	0,015	0,015	0,016	0,015	0,017	0,024	0,056	0,047	0,068	0,029	0,028	0,034
$R_{average}$ [Ω]		0,015			0,019			0,057			0,030	

Energy estimation

Using equations (2) and (3) was estimated the energy applied by the first positive semi-cycle of each one current signal applied. The average resistance obtained from the first three impulses was taken as the fabric resistance. The energy (in joules) related to the current (in kiloamperes) on each weave pattern is shown in Fig. 9.

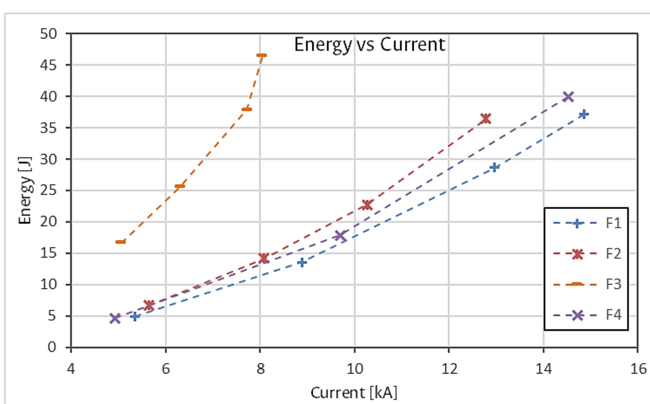

Figure 9. Energy-Current averages of the subsequent lightning-type current tests over four conductive fabrics.

After the second applied lightning impulse current, a slight change in the color of the fabrics was noticed. From the original silver color, the surface acquires a soft dark tone.

This suggests overheating of the material probably due to the joule heating produced by the lightning impulse current which could sublimate the thin conductive metallic layers when the current density surpass a critical value of current density. With enough high current applied, the conductive layer of the fabric structure changes because it loses some of the conductive material layer in some areas. This increases the electrical resistance and therefore the energy applied by the current source for the subsequent impulses. In a previous work, for a dog-tag metallic chain (i.e. pearl-like necklace) was assessed a critical current of 17,4 kA peak of a 8/20 µs waveshape, for the sublimation and break down of the material [27]. For the textile samples tested the more the lightning current impulse amplitude, the more the effect on the fabric surface was observed. Fig. 10 shows a representative sample of each one material of Table I, after the application of the last lightning impulse current.

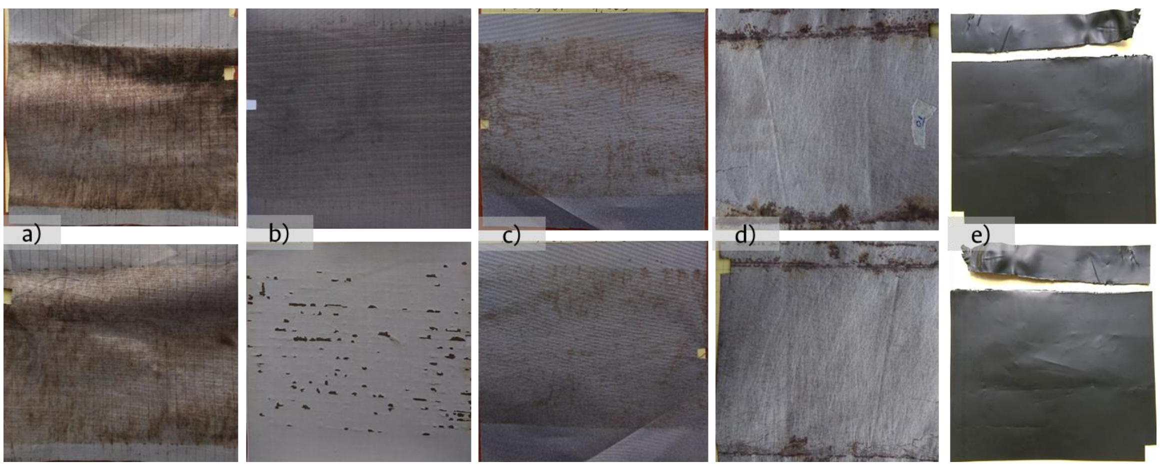

Figure 10. Samples of each textile F1 (a), F2 (b), F3 (c), F4 (d) and the polymeric film F5 (e) after some impulsive current tests. The textiles (F1 to F4) shows marks in the front and back surfaces, and the film (F5) shows the cut due the melting of the material. Note the flame retardant material in the back surface of F2 (b) with horizontal scratches perpendicular to the crossing current.

Moreover, some other lightning impulse current tests were performed considering the possible use of conductive fabrics as part of a protective mobile shelter against lightning. In this case, a test was performed with the LICG setup on a model made from fabric F1 (of the rip-stop type). The layout of the OUT was a fabric folded and sewn in a configuration of A-frame tent type which would be an outdoor tarp tent, scaled to 1:10. The ridge of the tent model was struck with two subsequent 13,7 kA lightning impulse current, with a five minutes interval between them. The “burned” marks in the surface of that fabric left a web-like pattern, concentric to the entry point of the impulse current, as shown in Fig. 11 b) and c).

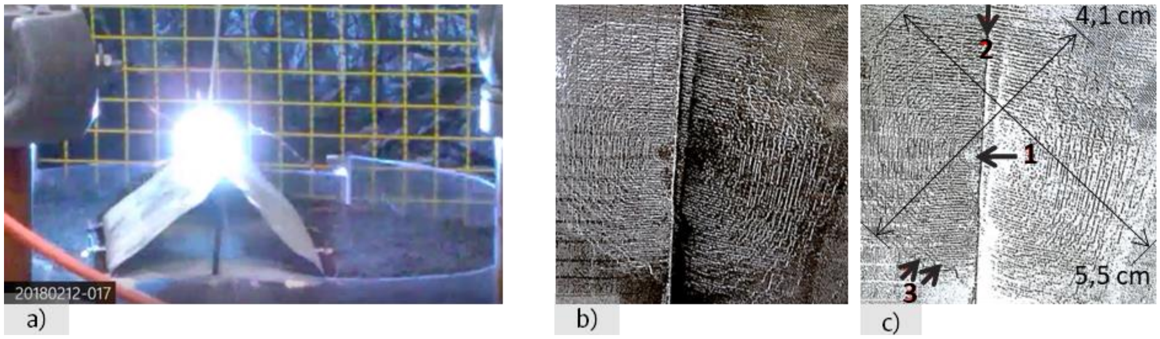

Figure 11. Ligthning impulse current test of 13,7 kA over an A-frame 1:10 scaled tent model (a) made with F1, left web-like pattern marks, easy visibles in the positive (b) and negative (c) images of a section of the rip-stop fabric. The lightning impulse current applied in the point (c 1) over the ridge of the tent model (c 2) left concentric marks (c-3).

SEM Inspections

To assess the morphology changes on the OUT fabrics after the lightning current tests, some selected samples were observed by means of Scanning Electronic Microscope (SEM). The magnification was increased over some scratches on the surface as shown in Fig. 12.

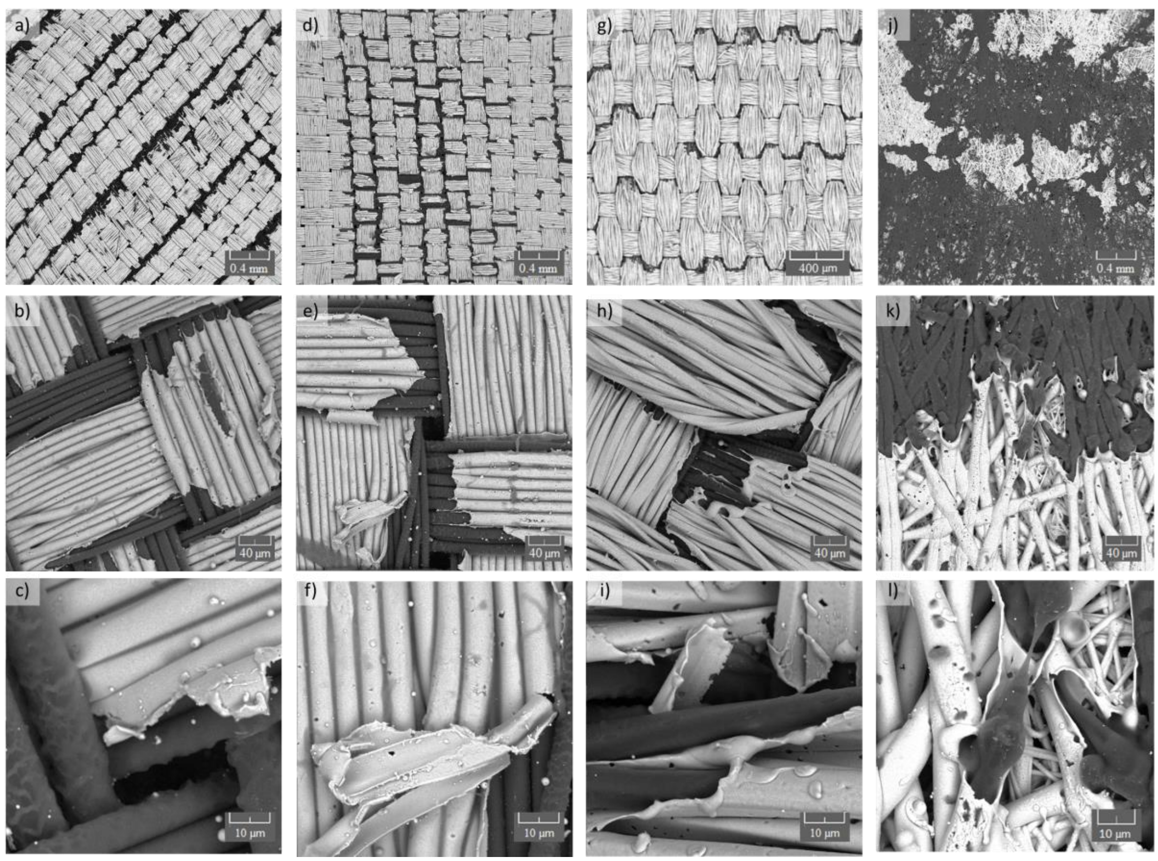

Figure 12. SEM micrographs (HV: 20.0 kV) of the textile samples of the four conductive fabrics after the lightning impulse tests: a), b) and c) rip-stop; d), e) and f) rip-stop with a side coated with a flame-retardant; g), h) and i) plain-weave, and j), k) and l) non-woven type.

The secondary electron image detection (SEI) of the SEM microscopy allows easy identification of the conductive and non-conductive materials, mainly because the atomic number of metal atoms are greater than those of nonconductive organic compounds. The dark areas of the non-conductive polymer fibers contrast strongly with the clear areas of the conductive metallic coating. Under the conditions described, SEM micrographs show optically that the woven fabrics (F1, F2 and F3) would better support the high-currents flow. This suggests that the woven type has a better performance to endure the current flow, i.e. the most ordered and straight the weave the more its capacity to drive impulsive currents. However, this observation could depend on the length, the material and the production technique of the fibers of non-woven fabrics.

With the SEM Energy Dispersive Spectrometry analysis (SEM-EDS), the estimation of the elemental composition of the conductive surface layer was performed over a sample of F1 rip-stop fabric. The SEM-EDS analysis identified a composition of 55% Cu - 45% Ni over a non-affected spot area of the fabric surface, as shown in Fig. 13 a). In the same way, over the observation region of the F1 surface after lightning current tests, was identified a elemental composition of 44% Cu - 36% Ni - 16% O - 4% C, as shown in Fig. 13 b), where carbon and oxygen are two basic elements of the inner polyester fibers.

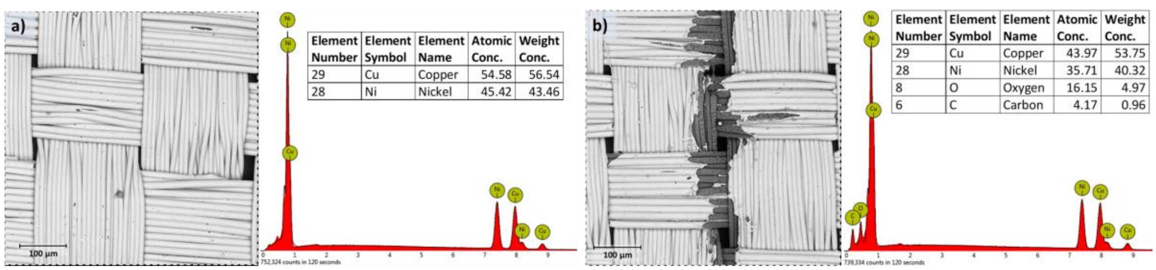

Figure 13. SEM-EDS elemental composition analyses before (a) and (b) after lightning current tests on F1 fabric.

Loss of material and "crosswise asperities"

Because of the melting and sublimation of the outer metallic layer of the yarns, the conductive material is lost in some regions of the fabric surface. In this case the polyester base material of the fiber core is exposed and can be recognized as some dark patterns presented in previous figures (Figs. 7, 10, 11 and 12). This loss of material results in loss of weight. Table III shows the weights taken for each of the fabric samples before and after tests, revealing an average loss of approximately 0,8% for F1 (ripstop), 23,2% for F3 (ripstop + flame retardant), 0,4% for F2 (plain weave), and 0,7% for F4 (non-woven). Particularly, F3 shows the greatest loss, due also to the release of small pieces of the flame-retardant layer composite, following the pattern of scratches left on the conductive fabric surface.

TABLE III. WEIGTH LOSS FOR ELECTROCONDUCTIVE FABRIC SAMPLES OF 10 X 10 CM BEFORE AND AFTER TESTS

	Before	**After**	**Difference**	**%**
Sample	[g]	[g]	[mg]	
F1-1	0,8244	0,8170	7,4	0,9
F1-2	0,8330	0,8290	4,0	0,5
F1-3	0,8274	0,8202	7,2	0,9

F1-Avg	*0,8283*	*0,8221*	*6,2*	***0,8***
F2-1	2,4377	1,9185	519,3	21,3
F2-2	2,3962	1,9118	484,4	20,2
F2-3	2,3342	1,6779	656,2	28,1
F2-Avg	*2,3894*	*1,8361*	*553,3*	***23,2***
F3-1	1,2124	1,2075	4,9	0,4
F3-2	1,2001	1,1950	5,2	0,4
F3-3	1,2012	1,1958	5,4	0,5
F3-Avg	*1,2046*	*1,1994*	*5,2*	***0,4***
F4-1	0,7573	0,7513	5,9	0,8
F4-2	0,8180	0,8129	5,1	0,6
F4-3	0,7983	0,7920	6,4	0,8
F4-Avg	*0,7919*	*0,7861*	*5,8*	***0,7***

Considering the fabric as a simple homogeneous conductive surface, the loss of material, due to the conduction of a high lightning current, leaves some scratches or "crosswise asperities" that constrain the conduction of the electrical current to certain remaining paths, in similar way to the interface between two bulk electrical contacts. Fig. 14 shows a sequence representation of the crosswise asperities on the conductive textile surface. The remaining "contact paths" after the lightning impulse current test can provide the conducting routes for the electrical current flow of subsequent discharges, considering that a lightning flash could have more than a single stroke [28].

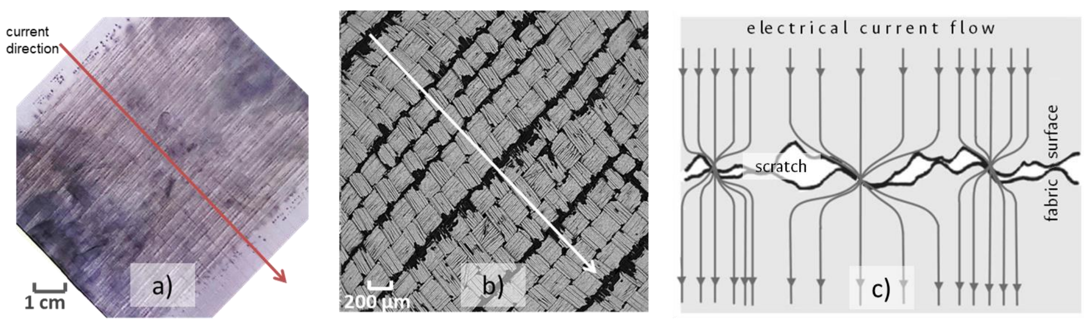

Figure 14. The lightning impulse currents produce scratches marks on the surface of the fabric (a and b) perpendicular to the current direction. Free interpretation of the crosswise asperities at the contact interface on a conductive fabric surface scratch (c) after lightning impulse current test (a and b [25], c: adapted from [29]).

For subsequent discharges, the scratch is itself an interface between neighbor conductive areas that determines the paths that can effectively conduct new currents. Remaining conductive paths continue to drive currents and open ways cannot do it. However, in absence of these conductive paths and with enough high electric potential, the conductive meeting areas can be sufficiently close to facilitate the breaking of air dielectric strength between them, sparking, jumping and conducting the currents through the surface. Depending on the shape and size of the electrodes, pressure, and moisture of the air, in laboratory conditions, the dielectric strength of air is about 3 kV/mm (3 V/µm).

Discussion

The samples of four different weaves tested show a tendency to burn up more easily crosswise, perpendicular to the current flow, and left on the surface fabric horizontal scratches probably due to overheating, melting or vaporization of the metallic coatings of the yarns. It was observed that the mentioned crosswise scratches, shown in Figures 7 and 10 to 14, are more noticeable at larger currents. Figs. 11 b) and 11 c) shows a concentric pattern that forms a web-like design on the surface of the fabric. In this, assuming the even distribution of the current from the contact point towards the outside, the scratches appear perpendicular to the current flow. In non-woven fabric F4, as shown in Fig 7, 10 and 12, is marked the horizontal melting effect not only as lines but also as large areas following a perpendicular pattern.

The resistance value of the electroconductive fabric is a key parameter of the electroconductive fabric intended to drive lightning currents. The elemental composition of the yarns conductive layer defines the resistivity, therefore the resistance. According to the SEM-EDS analysis (Fig. 13), the tested fabrics in this research are made from yarns with a conductive layer of copper-nickel alloys in a concentration of approximately 55% Cu and 45% Ni. The resistive of the fabric depends on the conductive material used in the fabric yarns. Carbon fibers, carbon nanotubes (CNT), graphene-coatings, and other non-metallic conductive materials based on organic compounds have relatively high resistivities compared with metallic ones, such a copper, leading to higher resistance values and therefore, greater energy dissipation in heat form. However, it is possible that bundling many yarns of materials with enough low resistivity can lead to a weave with low resistance able to withstand lightning currents. The polymeric carbon-coated film F5 indicated at the beginning of this study, shows that cannot withstand even a single 5 kA lightning impulse, because the heat generated melt the material itself along the contact electrode.

As shown schematically in Fig.1 and through micrographs of Fig. 3 and 12, the metal layer on the yarn of the fabric forms a tube net that can conduct lightning impulse currents. Despite the loss of conductive material by melting in initial lightning impulse current tests, the fabric continues conducting through the remaining paths in the subsequent lightning impulse currents, losing more of the metal coating. The SEM micrographs of Fig. 12 l) even reveal the non-conductive polyester core base fiber melted, out of the little tubes formed by the metal sheath around it. The weight change consequence of the melting and loss of material after lightning tests, presented in Table III, does not suggests any relation with the capacity of the electroconductive fabric to withstands the laboratory lightning currents. The greatest weight loss (23,2%) was in the F2 rip-stop fabric with FR layer and the lowest loss (0,4%) in the F3 plain-weave, the latter with the worst electric result. Thus, this result can be related most with the mechanical effect and would only indicate the loss of material in the air, suggesting that not necessarily the lost material goes out of the weave and could remain tangled up in the fabric yarns, as shown in Fig. 12 i).

The final damage of the flame-retardant coating composite on the side back, and the surface marks on F2, suggest that the composite help to increase the physical strength of the fabric against lightning current damage possibly due to the increased capacity of the coating to support higher temperatures. However, the composite layer could increase the electrical resistance as shown in Fig. 8 and Table II. Additionally, the composite layer increases the stiffness, weight and thickness of the conductive fabric, hindering its manageability.

Crosswise asperities produced on the conductive surface of the fabrics remain able to conduct electrical currents but increasing the resistance of the material, as shown in Fig. 8 for the four fabric types, where its value has a considerable change after the third lightning impulse current. For these fabrics, a resistive behavior can be considered until the third impulse which current value depends on fabric itself. However, the fabric F3 (plain-weave) shows a strong change in sample 2 (F3-2) after the 8 kA impulse, reducing the current value but increasing the voltage. At 8 kA gives a resistance of 69 mΩ and for the next current value of 7,5 kA gives a resistance of 141 mΩ. A higher current value was expected at this point, but the output current of the generator setup is determined by the impedance of the fabric. This unexpected point in F3-2 response shows that F3 fabric has a critical value of current conduction, as also F3-1 and F3-3 present despite the little shift between them. This change suggests that there is more than one conduction mechanism in the conductive fabric.

The obvious conduction mechanism is the flow of current through the material of the conductive surface itself, as inferred for the first three impulses. For subsequent discharges above this, the scratch becomes an interface between neighbor conductive areas determining the paths that can effectively conduct new currents. Remaining conductive paths continue to drive currents and open ways cannot do it. On the other hand, as said before in absence of conductive paths in the crosswise asperities, the electric potential can be enough high at the open meeting areas, enabling the breaking of the air dielectric strength between them producing sparks, bridging and conducting lightning currents through the previously electrically open surface.

The resistive behavior displayed in the Current-Voltage plots of Fig. 8 for the fabrics F1, F2 and F4, is extended to higher current values suggesting that, at least electrically, these textiles support better the lightning currents. For all tested fabrics, the three first impulses have an approximate linear ohmic resistive behavior, after which the yarns change enough their structure to modify permanently the weave, implying an alteration in the electrical current conduction mechanism, in a similar way to expressed in the paragraph before. There is not enough evidence from the outcomes of the tests to conclude that subsequent lightning impulses of currents below a critical peak value can produce progressive damage in the fabrics. Conversely, it can be said that above this critical value show by the third impulse of current, the scratches are more marked and the damage is progressive, as each time fewer and fewer conductive paths remain.

The characteristic Energy vs Current plotted in Fig. 4, shows an evident difference for the fabric F3. The energy estimation was done with the first peak current applied for the first three impulses in the four F1 to F4 fabrics, reveling a similar behavior for the fabrics F1, F2 and F4 against lightning currents. This shows that the plain-weave electroconductive textile F3 dissipates more energy at lower current values, consistent with their electrical resistance presented in Table II, greater than for the other three types.

Woven type textiles comprise weave patterns according to its final use. The rip-stop fabric has a special weave array with a reinforcing technique that makes them mechanically resistant to ripping and tearing. Conversely, the nonwoven fabric appears more fragile with a paper-like brittle feature. Despite the similar energy-current and voltage-current characteristics between F1 and F4 against lightning impulses, fragility is an undesirable attribute.

Fig.12 SEM micrographs show that the nonwoven fabric surface (F4) has regions that endure worse the high-currents flow despite to their electrical response and visual aspect.

This suggests that the woven type has a better performance to endure the current flow, i.e. the most ordered and straight the weave the more its capacity to drive impulsive currents. However, this observation could depend on the length, geometry, the material and the production technique of the fibers in non-woven fabrics. Furthermore, the F3 plain-weave with a pattern like that of the F1 and F2 rip-stop but with a loose weave, shows a greater resistance and consequently greater energy dissipation. Despite similar research is needed over knitting fabrics and this weave type is not treated in this work, considering they have a more intricated weave pattern that change the yarn paths, it could be expected less performance.

The horizontal scratches, perpendicular to the current flow, appear because of the overheating of metallic outer layer of the yarns by the Joule effect. Even though it is not totally clear how the horizontal pattern is produced, it is possible gives an explanation thinking the electroconductive tested fabrics as a tube conductive network. When a lengthwise current flow through a single tube, and this tube experiences a change in the direction, the current density inside increases or decreases according to the change which is subjected, analogous to a pipe that transport liquids. Where the current density increases, the heating increases as a consequence of the Joule effect and, conversely, when the current density decreases, the heating decreases. As the fabric has a symmetrical array multiply by much, it is produced the scratch pattern crosswise to the current flow. This concords with the observation of the previous paragraph that relates ordered and straight weaves with increased capacity to drive impulsive currents. According to this, it is possible that a perfectly smooth, plain and straight nonwoven fabric (similar to F4) with most long fibers oriented lengthwise to the current flow could withstand higher electric currents despite their fragility.

Furthermore, considering the lightning parameters given in Tables A.1 and A.3 of IEC62305-1 [7], the 50% value of a typical first negative stroke corresponds to a current of 20 kA peak and it has a probability P=0,8. This suggest the possibility to conform lightweight and portable LPS. Additionally, it is very important to remember that both direct and indirect lightning impulse currents of natural atmospheric discharges cause injuries. In fact, a larger number of fatal accidents are caused by step potentials, despite its low intensity currents, but sufficient to produce cardiorespiratory arrest [30]. Further study is necessary on this subject to have more accurate information.

Despite the disadvantage of the metal-coated yarns that may be peeled off due to washing or other types of mechanical abrasion [12], [15] , considering only the visible and electrical effects of the lightning currents on the tested fabrics and discarding those mechanical, the rip-stop weave has proven to be a tough material with better performance to support lightning impulse currents like those produced by electrical atmospheric discharges.

Conclusion

Four types of conductive fabrics and a carbon-impregnated polymeric film were tested by triplicate in high-voltage laboratories. Four consecutives laboratory lightning-type currents to simulate natural lightning strikes were applied to 10 cm x 10 cm samples of rip-stop, plain-weave and nonwoven fabrics, and over a polymeric carbon impregnated film. Moreover, a tent scaled model was subjected to two subsequent lightning impulses of about 14 kA. Mechanically, the tested fabric samples withstand the trials with progressive increasing currents except the carbon impregnated film. Electrically for the fabrics, it was observed an ohmic resistive behavior until a certain critical value for each fabric type, from which the current-voltage characteristic change. The microscopy inspections reveal that the patterns left by the lightning impulse currents on the fabric surfaces are due to the melting of the outer conductive layer deposited over the nonconductive fibers core. Electroconductive fabrics with minimum sheet resistance values are desirable to withstand high lightning currents. The results of this experimental research suggest that is possible to use rip-stop conductive fabrics in lightweight and portable Lightning Protection Systems to mitigate lightning risks in outdoor applications such as tents and mobile shelters.

Acknowledgment

The authors want to thank the Universidad Nacional de Colombia and their professors for all the help and support, access to SEM and use of HV laboratories, Francisco Amortegui and Fernando Herrera from the LABE and the Electric and Electronic Department. We also thank Jorge Ignacio Villa who is pursuing the Doctorate in Sciences – Physics, at the Sciences Department. This research is partially supported by the Administrative Department of Science, Technology and Innovation of Colombia – COLCIENCIAS through the grant of *Convocatoria 647 de 2014* and through the Project No.37658/2017 of the *Convocatoria Nacional de proyectos para el fortalecimiento de la investigación, creación e innovación de la Universidad Nacional de Colombia 2016-2018*.

References

[1] R. I. Albrecht, S. J. Goodman, D. E. Buechler, R. J. Blakeslee, and H. J. Christian, "Where Are the Lightning Hotspots on Earth?," *Bull. Am. Meteorol. Soc.*, vol. 97, no. 11, pp. 2051–2068, Feb. 2016.

[2] N. Navarrete-Aldana, M. A. Cooper, and R. L. Holle, "Lightning fatalities in Colombia from 2000 to 2009," *Nat. Hazards*, vol. 74, no. 3, pp. 1349–1362, May 2014.

[3] J. A. Cristancho C., J. J. Pantoja, C. Rivera, and F. Roman, "Analysis of two nonfatal lightning accidents in Colombia," *Electr. Power Syst. Res.*, vol. 153, pp. 159–169, Dec. 2016.

[4] K. M. Walsh, B. Bennett, M. A. Cooper, R. L. Holle, R. Kithil, and R. E. López, "National Athletic Trainers' Association Position Statement: Lightning Safety for Athletics and Recreation," *J. Athl. Train.*, vol. 35, no. 4, pp. 471–477, 2000.

[5] OSHA-NOAA, "Lightning Safety When Working Outdoors," *FactSheet*, vol. FS-3863, p. 5, May 2016.

[6] C. Cruz, E. Rentería, and F. Román, "Statistics of the Colombian National Army lightning accidents," in *2013 International Symposium on Lightning Protection (XII SIPDA)*, 2013, pp. 324–328.

[7] IEC 62305-1, *Protection against lightning - Part 1: General principles*, vol. IEC 62305-1:2010. 2010.

[8] Christian. Bouquegneau, "External lightning protection system," in *Lightning Protection*, V. Cooray, Ed. London, UK: The Institution of Engineering and Technology, 2010.

[9] National Fire Protection Association, *NFPA 780 - Standard for the installation of Lighting Protection Systems - 2017*, NFPA. 2017.

[10] R. H. Golde and W. R. Lee, "Death by lightning," *Proc. Inst. Electr. Eng.*, vol. 123, no. 10, pp. 1163–1180, Oct. 1976.

[11] Messe Frankfurt, "Techtextile Application Areas," *Techtextile Application Areas*. [Online]. Available: https://techtextil.messefrankfurt.com/frankfurt/en/besucher/messeprofil/anwendungsbereiche.html?nc. [Accessed: 14-Mar-2018].

[12] A. M. Grancarić *et al.*, “Conductive polymers for smart textile applications,” *J. Ind. Text.*, vol. 48, no. 3, pp. 612–642, Sep. 2018.
[13] W. C. Smith, *Smart Textile Coatings and Laminates*. Woodhead Publishing, 2010.
[14] M. Miao and J. H. Xin, *Engineering of High-Performance Textiles*. Woodhead Publishing, 2017.
[15] T. Dias, Ed., *Electronic Textiles: Smart Fabrics and Wearable Technology*, 1 edition. Woodhead Publishing, 2015.
[16] Zhejiang Saintyear Electronic Technologies Co., Ltd., “Structure of conductive fabric,” 11-Nov-2017.
[17] A. Dhawan, A. M. Seyam, T. K. Ghosh, and J. F. Muth, “Woven Fabric-Based Electrical Circuits: Part I: Evaluating Interconnect Methods,” *Text. Res. J.*, vol. 74, no. 10, pp. 913–919, Oct. 2004.
[18] J. Banaszczyk, A. Anca, and G. D. Mey, “Infrared thermography of electroconductive woven textiles,” *Quant. InfraRed Thermogr. J.*, vol. 6, no. 2, pp. 163–173, Dec. 2009.
[19] Y. Zhao, J. Tong, C. Yang, Y. Chan, and L. Li, “A simulation model of electrical resistance applied in designing conductive woven fabrics,” *Text. Res. J.*, vol. 86, no. 16, pp. 1688–1700, Oct. 2016.
[20] S. Varnaitė-Žuravliova, J. Baltušnikaitė-Guzaitienė, L. Valasevičiūtė, R. Verbienė, and A. Abraitienė, “Assessment of Electrical Characteristics of Conductive Woven Fabrics,” *Am. J. Mech. Ind. Eng.*, vol. 1, no. 3, p. 38, Oct. 2016.
[21] ASTM F390-11, *Test Method for Sheet Resistance of Thin Metallic Films With a Collinear Four-Probe Array*. 2011, p. 5.
[22] ASTM D4496−13, *Test Method for D-C Resistance or Conductance of Moderately Conductive Materials*. 2013.
[23] CIGRE WG C4.407, *Lightning Parameters for Engineering Applications*. 2013, p. 118.
[24] H. E. Rojas, F. Santamaría, O. F. Escobar, and F. J. Román, “Lightning research in Colombia: Lightning parameters, protection systems, risk assessment and warning systems,” *Ing. Desarro.*, vol. 35, no. 1, pp. 240–261, Jun. 2017.
[25] J. A. Cristancho C., J. E. Rodriguez M., C. A. Rivera G., F. Roman, and J. J. Pantoja, “High Current Tests over Conductive Fabrics,” in *2018 International Conference on Electromagnetics in Advanced Applications (ICEAA)*, 2018, pp. 428–432.
[26] E. Kuffel, W. S. Zaengl, and J. Kuffel, *High Voltage Engineering Fundamentals*. Oxford: Newnes, 2000.
[27] J. A. Latorre, J. E. Rodriguez, C. A. Martínez, J. A. Cristancho C., and F. Román, “Characterization of a Metallic Pearl-like Necklace stroked by lightning: preliminary results,” in *2016 International Conference on Lightning Protection*, Estoril, Portugal, 2016.
[28] V. A. Rakov *et al.*, “CIGRE technical brochure on lightning parameters for engineering applications,” in *2013 International Symposium on Lightning Protection (XII SIPDA)*, 2013, pp. 373–377.
[29] P. Gharghabi, J. Lee, T. Colmer, M. S. Mazzola, T. E. Lacy, and J. Kluss, “Investigating the Composite/Metal Interface and its Influence on the Electrical Resistance Measurement,” *ArXiv180406246 Phys.*, Apr. 2018.
[30] M. A. Cooper, C. J. Andrews, R. L. Holle, R. Blumenthal, and N. Navarrete-Aldana, “Lightning related-injures and safety,” in *Auerbach’s Wilderness Medicine*, 7th edition., P. S. Auerbach, Ed. Philadelphia, PA: Elsevier, 2016, pp. 71–117.